



# Laser ablation in a model two-phase system

Gareth J. Williams<sup>a,\*</sup>, Leonid V. Zhigilei<sup>a,b</sup>, Barbara J. Garrison<sup>a</sup>

<sup>a</sup> Department of Chemistry, 152 Davey Laboratory, The Pennsylvania State University, University Park, PA 16802-6300, USA

<sup>b</sup> Department of Material Science and Engineering, Thornton Hall, University of Virginia, Charlottesville, VA 22903, USA

---

## Abstract

Short pulse laser ablation of a model two-component system has been simulated using a coarse-grained molecular dynamics (MD) model. A system with two disparate components (hard and soft) has been considered, based broadly on the properties of hard tissue. The existence of distinct regimes of material ejection has been identified and the processes leading to the ablation have been investigated. In the lower fluence regime gaseous particles of the soft component stream from the hard matrix but there is no ejection of the hard component. In the higher fluence regime chunks of the hard component are ejected simultaneously with the soft component. © 2001 Elsevier Science B.V. All rights reserved.

*PACS:* 61.80.Ba; 82.20.Wt; 42.62.Be; 02.70.Ns

*Keywords:* Molecular dynamics and particle methods; Laser ablation of hard tissue

---

## 1. Introduction

Laser ablation is an increasingly important technological process [1]. Material ejected from an irradiated target may be used in thin film deposition [2] or mass-spectrometric analysis [3]. When laser ablation is used in surgical applications [4,5], rather than a basic picture of what is happening on a microscopic scale during ablation, the rate of material removal and the properties of the surface left behind is the primary focus. One successful approach for obtaining a microscopic view is molecular dynamics (MD) simulations using the breathing sphere model [6,7]. For this work, the

breathing sphere model has been modified to treat a two-phase system with drastically different properties of the component materials in order to provide a basic picture of laser ablation of a two-phase system.

## 2. Model system

Part of the motivation for this work comes from considering the surgical application of laser ablation for cutting hard tissue (bones and teeth). In developing the model system for this work we have attempted where possible to make our system broadly comparable with hard tissue. Hard tissue is inhomogeneous down to microscopic dimensions and has a composite structure with major constituents being the relatively soft and elastic

---

\* Corresponding author. Tel.: +1-814-863-2108; fax: +1-814-863-5319.

E-mail address: gareth@chem.psu.edu (G.J. Williams).

collagen and hard crystalline apatite. The smallest dimension structure in hard tissue is not understood in detail. What is known of the structure is that the collagen forms an arrangement of aligned microfibrils, and some of the apatite exists in microcrystallites of about 4–40 nm size [8]. Further, the two components each occupy about equal volumes. For this study highly idealized soft and hard components occupying equal volumes are considered, with structure on a similar length-scale to hard tissue, but without attempting to model any detailed microstructure of hard tissue.

In the breathing sphere model [6] materials are made up of spherical particles. The radii of the particles are allowed to vary (the particles “breathe”) governed by an “internal” potential and assigned inertial parameter. The particles interact with one another through simple pair potentials, which act between their surfaces. A summary of the main inter-particle potential parameters and approximate resultant material properties appears in Table 1. For the potential between particles of the hard and soft types, the same parameters as for the hard material potential were used, except for a smaller value for  $U_0$  of 0.1016 eV. The properties of these highly idealized materials are difficult to compare closely with the actual constituents of hard tissue. For example, collagen does not have simple behavior on heating and cannot be said to actually have a melting point.

In the breathing sphere model a single material has a heat capacity per particle, fixed by the degrees of freedom of the system (3 translational, 1 internal). To provide the particles of the model with an appropriate heat capacity, the breathing sphere model has been extended to add an internal energy

bath to each of the particles in the model. Each internal bath has a fixed heat capacity (to make the total heat capacity up to values of 0.79 and 1.4 J/g/K for the hard and soft components) and contains a variable energy, which may be identified with a temperature. The internal bath is made to couple with the breathing mode, which in turn coupled with the translational modes of the system. The bath–breathing coupling is implemented in the form of a velocity dependent damping (driving) force acting on the breathing motion. The damping coefficient is set to make the temperature of the breathing motion and the internal bath approach one another. These temperatures are defined in terms of the amount of energy in the different modes (time averaged for the breathing kinetic energy) and their heat capacity. The amount of energy transferred to/from the baths is calculated in terms of the work done by the damping forces. With this new element of the breathing sphere model, photons from the laser pulse may be simply deposited into the internal baths.

Input parameters to control the breathing mode, and coupling to the internal bath were chosen to give a characteristic energy transfer time between internal modes and translation of 10 ps. (For the soft and hard materials respectively the parameters chosen were the ratio of internal inertial parameter to particle mass of 1:1 and 16:1, the second derivative of the harmonic internal potential of 0.75 and 11.385 eV/Å<sup>2</sup> and the time constant for transfer of energy between bath and breathing in isolation of 1 and 3 ps.)

The preparation of two-phase samples to be used in the ablation simulation consisted of the following steps. First, small periodic ( $15 \times 15 \times 15$  nm<sup>3</sup>) single

Table 1

Parameters used for the inter-particle potentials and some of the physical properties of the resultant hard and soft materials<sup>a</sup>

	$m$ (amu)	$U_0$ (eV)	$\alpha$ (nm <sup>-1</sup> )	$r_0$ (nm)	$r_{\max}$ (nm)	$R_0$ (nm)	$\rho$ (g/cm <sup>3</sup> )	$c$ (m/s)	M.P. (K)	$B$ (Gpa)
Hard	70	0.254	15.45	1.94	5.0	0.906	3.15	4000	2000	50
Soft	100	0.04	10	3.0	10.0	1.4	1.22	1200	330	2.6

<sup>a</sup>  $U_0$ ,  $\alpha$  and  $r_0$  are parameters of the Morse potentials used,  $U(r) = U_0(\exp(-\alpha(r - r_0)) - 1)^2$ . The potentials are smoothly cut-off to zero by  $r_{\max}$ . The particles have equilibrium radius  $R_0$  and mass  $m$ . The resultant materials have density  $\rho$ , speed of sound  $c$ , melting point M.P. and bulk modulus  $B$ .

component samples of the hard and soft materials were prepared at room temperature. The particles in the soft component were then assigned at random between two groups in order to define a fine-grained two-phase structure. Then this fine-grained structure was consolidated into a coarser-grained two-phase structure. The consolidation was done by swapping particle types based on the number of like-type neighbors within a cutoff radius (containing up to about 15 neighbors), in a Monte-Carlo fashion, with probability highly weighted for particles with the least like-type neighbors to be swapped. The total number of accepted swaps was used to control the coarseness of the resulting structure. This method was used to allow generation of a two-phase structure with relatively low surface energy for its granularity, without imposing

arbitrary prejudice. The final sample consists of two inter-twined matrices. One of the groups of soft particles was chosen to form the soft material in a two-component two-phase sample, with particles from the sample of hard component incorporated in the remaining space. The resultant structure had considerable excess interfacial energy. The sample was enabled to seek a low energy configuration via MD simulations with temperature and pressure control. Before running simulations of ablation, the  $15 \times 15 \times 15 \text{ nm}^3$  sample was stacked to make a  $15 \times 15 \times 120 \text{ nm}^3$  sample with a surface in the long ( $z$ ) direction and a boundary layer of thickness 1.3 nm defined at the base of the sample. Non-reflecting boundary (NRB) [9] conditions were imposed to prevent pressure wave reflections from the base of the sample.

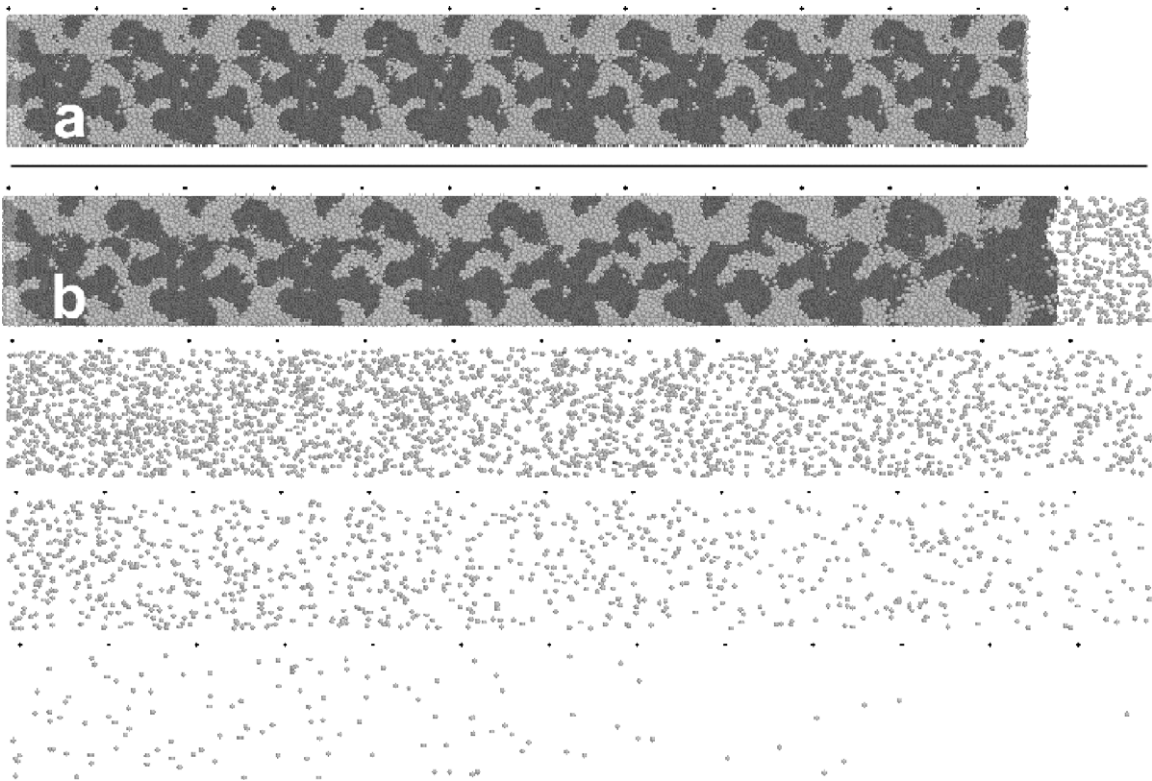


Fig. 1. (a) The initial configuration of the particles used in the simulations and (b) the configuration at 280 ps after a  $1 \times 10^{-2} \text{ J/cm}^2$  laser pulse. The hard component particles are darker and represented by smaller radius spheres. Here and in Fig. 2, particles in successive distance ranges from the base of the sample are offset from one another to show all of the particles. Particles in the boundary layer are colored lighter. Particles of the soft component are streaming from the hard matrix. Points are drawn at 10 nm intervals to indicate the scale.

Laser absorption was implemented in the simulation by depositing photons into the internal baths of particles with an appropriate spatial and temporal distribution. The laser absorption depth was set to be 50 nm and most of the simulations had a pulse duration 1 ps. The range of laser fluences was chosen so that interesting changes in the character of the ablation could be observed.

### 3. Results and discussion

In the simulations to be discussed, the laser fluences were 1, 1.5, 2 and  $3 \times 10^{-2} \text{ J/cm}^2$ . The lowest fluence will be considered first. The config-

uration of the particles at the start of the simulation and at a time of 280 ps from the laser pulse is depicted in Fig. 1. At this fluence, mostly particles of the soft component are ejected, with only two particles of the hard component ejected. The sequence of events during the simulation is as follows. First, the sample is locally heated with a Beer's law profile following the laser absorption, such that the temperature increases at the surface by 800 K up to 1100 K and the base of the sample by 100 K up to 400 K. There is local thermalization of energy on the length-scale of the two-phase structure on a time-scale of tens of picoseconds. The sample becomes in compression from the heating, and expands from the surface with a rarefaction pressure wave. Concurrently, some of the

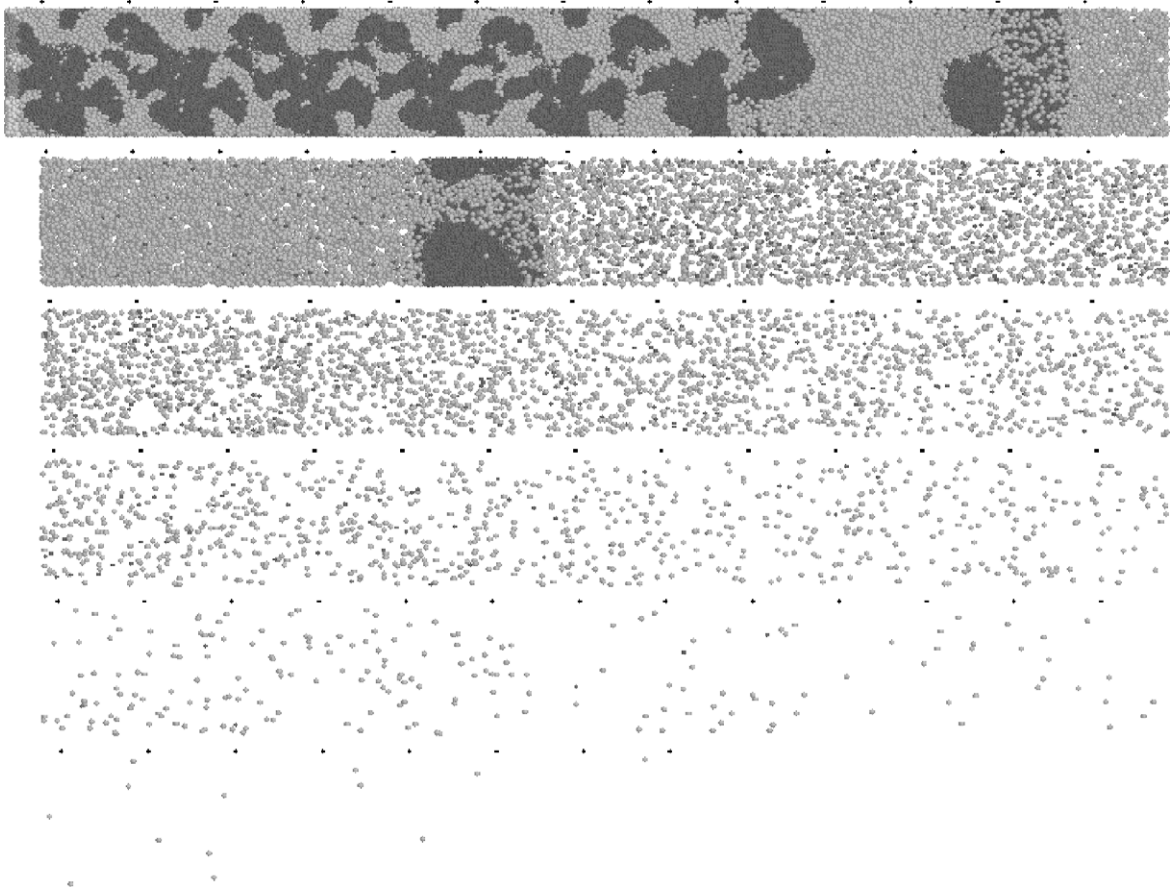


Fig. 2. The particle configuration at 280 ps after a  $2 \times 10^{-2} \text{ J/cm}^2$  laser pulse. Two large chunks of hard material are leaving the surface along with a plume of particles.

now gaseous soft component streams out from the hard matrix and forms a plume. The hard component does not change overly in structure except for some expansion and some distortion near the surface where a significant amount of the soft component has left. By 280 ps the hard component has ceased expanding at a significant rate. The surface temperature remains high and it is apparent that the gaseous soft component will continue to evolve from the hard matrix at much later times.

The character of the ablation is considerably different at each of the higher fluences considered as particles of the hard component ablated from the surface along with those of the soft component. The configuration of the particles at a time of 280 ps from the laser pulse for a fluence of  $2 \times 10^{-2} \text{ J/cm}^2$  is depicted in Fig. 2. In this case, the temperature rises at the surface by 1600 K up to 1900 K. As with the lower fluence, hot gaseous particles of the soft component stream from the

sample. There are also a significant number of single hard particles entrained in the plume. Simultaneously, there is ejection of chunks of hard component. The size of the chunks is comparable with the periodic dimensions in the simulation and is probably determined by the weakest interfaces in the sample. This onset of a collective mode of ejection of the hard material indicates the presence of a fluence threshold between the regimes of material ejection at the lower and higher fluences considered.

Another depiction of the particle configuration shown in Fig. 2, appears in Fig. 3. In this representation, the sample has been divided into eight layers so that the three-dimensional structure may be observed. Furthermore the particles are color-coded by their type and initial position within the configuration to show the amount of particle transport in the direction of the surface normal. It can be seen that there is considerable diffusive

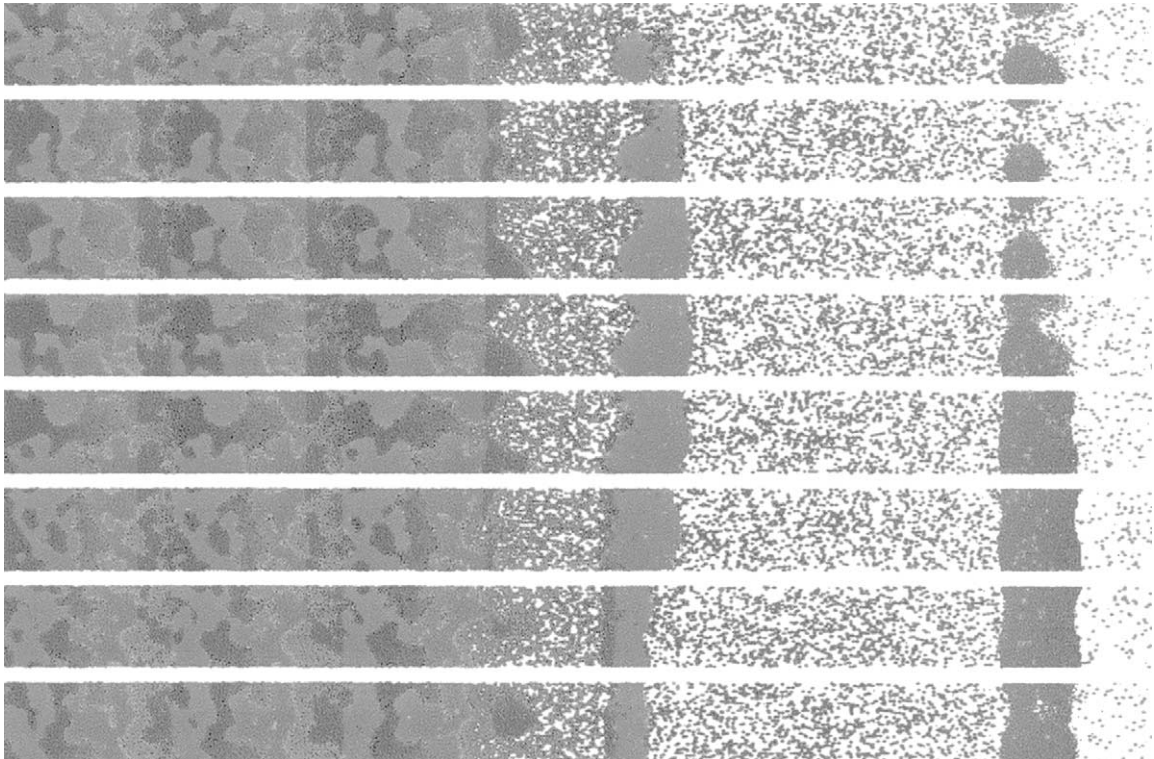


Fig. 3. The same configuration as in Fig. 2, with a restricted distance range. The particles are colored according to their types and initial position with the color cycling each 30 nm.

transport of the gaseous soft component and that it evolves out of the sample, flowing past the hard component structure. The hard component retains much of its structure in the lower part of the sample. In the chunks being ejected and the region of the new sample surface there is considerable deformation and consolidation of the structure. The time development of the particle configuration (not shown) indicates that the hard matrix does not break as a macroscopic brittle solid, but undergoes significant ductile deformation before it breaks. In a repeat simulation at  $2 \times 10^{-2} \text{ J/cm}^2$  with the same initial sample but with different particles absorbing the laser energy, the second chunk in Figs. 2 and 3 did not leave the surface.

The velocity profile for the simulation at  $2 \times 10^{-2} \text{ J/cm}^2$  at 280 ps is shown in Fig. 4. The two components in the plume have a common velocity at any given distance from the base of the sample, similar to the situation of ablating analytes embedded in a matrix [6]. The plume has an anisotropic velocity distribution with the velocity in the direction normal to the surface up to five times greater than the root mean square of the velocity components parallel to the plane of the surface.

With increasing fluence, a greater depth of the hard component becomes ablated. The hard component is ablated to depths of approximately 15, 15–30 and 45 nm for the 1.5, 2 and

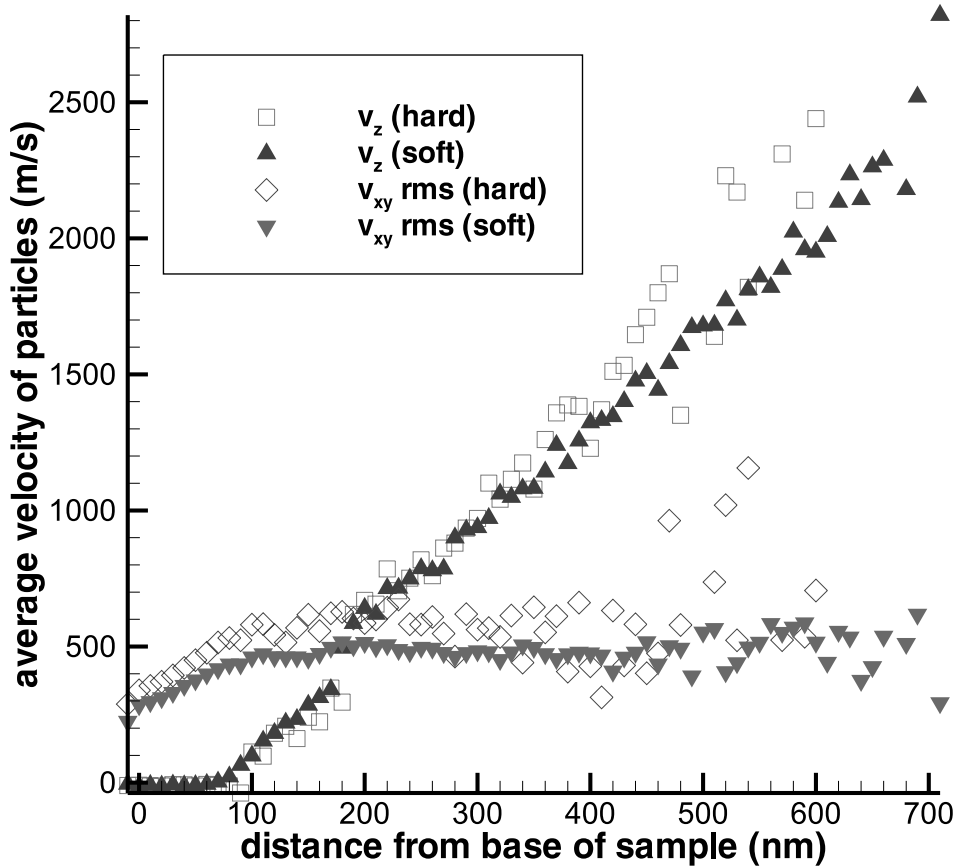


Fig. 4. The average velocity of particles of each component in different distance ranges from the base of the sample at 280 ps after a  $2 \times 10^{-2} \text{ J/cm}^2$  laser pulse. The average velocity in the direction perpendicular to the surface ( $v_z$ ) and the root mean square velocity in the plane of the surface ( $v_{xy} \text{ rms}$ ) are represented. At larger distances, the scatter in the averages is larger as there are fewer particles present to average over.

$3 \times 10^{-2} \text{ J/cm}^2$  fluences. At a fluence of  $3 \times 10^{-2} \text{ J/cm}^2$  the temperature increase at the surface is 2400 K, which is sufficient to melt the first large chunk ejected from the surface.

The breathing sphere model has proved successful in describing laser ablation under both thermal confinement and stress confinement regimes for a single component system [7]. In the stress confinement regime, tensile stresses can become sufficiently high to cause fracture in the sample and ablation of relatively cold chunks of material. In this work the characteristic time for stress relaxation is  $\tau_s \sim L_p/c \approx 33 \text{ ps}$ , with the laser penetration depth  $L_p = 50 \text{ nm}$  and speed of sound  $c \approx 1500 \text{ m/s}$ . The 1 ps laser pulse is shorter, so the ablation character might be expected to be dominated by the response of the sample to the sudden increase in compressive thermoelastic stress. However in this work, the two-component composition of the sample appears to cause the ablation to be dominated by the compressive stress due to the strong over-heating of the soft component. To test whether the laser pulse duration was of critical significance to the nature of the ablation, simulations at fluences of  $1.5$  and  $2 \times 10^{-2} \text{ J/cm}^2$  were repeated but with laser pulse durations of 50 ps. These simulations yielded essentially the same results as the simulations at the same fluences with 1 ps pulses. So, the ablation in the model system does not appear to depend on the laser pulse being particularly short, with ablation of the hard component not occurring until the fluence is high enough for the soft component to become a highly heated gas. Therefore, as long as this heating takes place before a significant amount of the gas escapes from being confined in the hard matrix, essentially the same character of ablation is anticipated.

#### 4. Conclusions

A microscopic picture of laser ablation of a two-phase material with inter-connected hard and soft components has been obtained. Two regimes

of material ejection have been identified. In both regimes, the deposited energy density is much greater than the minimum required to make the soft component become gaseous, and the soft component streams out of the hard matrix. In the lower fluence regime, there is little ablation of the hard component. In the higher fluence regime, the expansion of the soft component is sufficient to break off chunks of the hard material, which are entrained in a plume streaming away from the surface.

#### Acknowledgements

This work was supported by the United States Office of Naval Research through the Medical Free Electron Laser Program, and the National Science Foundation through the Chemistry Division. The computational support was provided by IBM through the Selected University Research Program, the National Science Foundation through the MRI program, and the Center for Academic Computing at Penn State University.

#### References

- [1] J.S. Horwitz, H.-u. Kerbs, K. Murakami, M. Stuke (Eds.), in: Proceedings of the Fifth Conference on Laser Ablation, Appl. Phys. A 69(Suppl.) (2000).
- [2] D. Bäuerle, Laser Processing and Chemistry, Springer, Berlin, 1996.
- [3] F. Hillenkamp, M. Karas, R.C. Beavis, B.T. Chait, Anal. Chem. 63 (1991) 1193.
- [4] G.M. Peavy, L. Reinisch, J.T. Payne, V. Venugopalan, Lasers Surg. Med. 25 (1999) 421.
- [5] S.L. Jacques (Ed.), Laser–Tissue Interaction XI: Photochemical, Photothermal, and Photomechanical, in: SPIE Proceedings Series Vol. 3914, SPIE, Bellingham, WA, 2000.
- [6] L.V. Zhigilei, P.B.S. Kodali, B.J. Garrison, J. Phys. Chem. B. 101 (1997) 2028.
- [7] L.V. Zhigilei, B.J. Garrison, J. Appl. Phys. 88 (2000) 1281.
- [8] J. Currey, The Mechanical Adaptations of Bones, Princeton University Press, Princeton, NJ, 1984.
- [9] L.V. Zhigilei, B.J. Garrison, Mater. Res. Soc. Symp. Proc. 538 (1999) 491.